

Special Issue of the 6th International Congress & Exhibition (APMAS2016), Maslak, Istanbul, Turkey, June 1–3, 2016

# Fabrication and Arc-Erosion Behavior of Ag<sub>8</sub>SnO<sub>2</sub> Electrical Contact Materials under Inductive Loads

S. BIYIK<sup>a,\*</sup> AND M. AYDIN<sup>b</sup>

<sup>a</sup>Karadeniz Technical University, Abdullah Kanca Vocational School,

Department of Machinery and Metal Technologies, 61530 Trabzon, Turkey

<sup>b</sup>Karadeniz Technical University, Department of Mechanical Engineering, 61080 Trabzon, Turkey

In this study, Ag-based SnO<sub>2</sub>-reinforced electrical contact materials were produced by powder metallurgy and mechanical alloying techniques. Elemental powder mixture containing 8 wt.% SnO<sub>2</sub> was milled in a high-energy planetary-type ball mill, to achieve homogeneously mixed composite powder, and subsequently pressed in a closed die to obtain green compacts with a cylindrical shape and then sintered under vacuum to obtain composites. Composites were then subjected to electrical wear tests under inductive loads to investigate the arc-erosion performance of electrical contacts. Surface deterioration and mass losses of electrical contacts were also evaluated, as a function of increasing switching number. Characterization of the starting and composite powders, green compacts, composites and arc-originated surface deterioration was carried out using scanning electron microscopy and energy-dispersive X-ray spectroscopy. It was found that powder particle size had decreased with the increasing milling time. Density and hardness values of the composites had increased, whereas porosity had decreased with the increasing sintering temperature. Optimum sintering temperature was determined as 900 °C. The arc-affected zones became bigger with the increase of the number of switching operations. Furthermore, comparison between surface morphologies and mass losses of arc-eroded specimens had revealed that the stationary contacts exhibit higher rates of erosion than the movable contacts.

DOI: [10.12693/APhysPolA.131.339](https://doi.org/10.12693/APhysPolA.131.339)

PACS/topics: 81.20.Ev, 81.70.-q, 07.50.-e, 84.32.Dd

## 1. Introduction

Electrical contacts are found in every electrical component, and the proper operation of the contacts is always vital to the reliable operation of that component. Therefore, electrical contacts should have certain characteristics. For example, silver-based composites reinforced with ceramic particles are widely used in electrical contact applications due to their superior combination of strength at elevated temperature, good thermal stability, high hardness, better anti-welding properties, and high electrical and thermal conductivity [1, 2]. The most common metal oxides used in electrical contacts are cadmium oxide (CdO), tin dioxide (SnO<sub>2</sub>) and zinc oxide (ZnO) [3–5]. Apart from this, refractory metals such as tungsten (W) and molybdenum (Mo) are widely used in Ag- or Cu-based electrical contacts [6].

To enhance arc-erosion performance of electrical contacts, manufacturing parameters should be optimized. Furthermore, studies are being performed with regards to improving the arc-erosion performance by using some minor doping additives, to form a ternary or complex composite, and extending the contact life [7–9]. Currently, Ag-SnO<sub>2</sub> composites have great potential in electrical contact applications due to their environmentally friendly nature, in contrast with the toxic and carcinogenic Ag-CdO electrical contact material. However,

arc-erosion behavior of Ag<sub>8</sub>SnO<sub>2</sub> contact material under inductive load has not yet been investigated in detail. Therefore, the primary purpose of the present study is to optimize manufacturing parameters of Ag<sub>8</sub>SnO<sub>2</sub> contact material and to investigate its arc-erosion behavior under inductive loads.

## 2. Experimental procedures

Elemental Ag (18.646 μm, 99.99% purity) and SnO<sub>2</sub> (10 μm, 99.9% purity) powders were used for mechanical alloying experiments (Fig. 1). Stearic acid was also added to powder mixture as a process control agent. Elemental powder mixture containing 8 wt.% SnO<sub>2</sub> was milled in a high-energy planetary-type ball mill with a milling speed of 300 rpm and a ball-to-powder weight ratio of 10:1, to achieve homogeneously mixed composite powder. The composite powder was then consolidated in a cylindrical die by applying a pressure of 350 MPa, followed by vacuum sintering at various temperatures, namely 700, 800 and 900 °C. After that, the physical and mechanical properties of the composites, such as green density, green porosity, sintered density, sintered porosity and microhardness were determined. Composites were then subjected to electrical wear tests using the arc-erosion test rig [10, 11], at an operating voltage of 220 V, a frequency of 50 Hz, and switching current of 20 A. The switching frequency and delay time were selected as 1 000 operations per hour and 2.6 s, respectively. Arc-erosion experiments were conducted under inductive loads for up to 40 000 operations. The mass-loss values of the electrical contacts were determined at every 5 000

\*corresponding author; e-mail: [serkanbiyik@ktu.edu.tr](mailto:serkanbiyik@ktu.edu.tr)

operations using a semi-micro-analytical balance with a precision of  $10^{-5}$  g. Surface deterioration and mass losses of electrical contacts were also evaluated as a function of increasing switching number. Characterization of the starting and composite powders, green compacts, composites and arc-originated surface deterioration was carried out using scanning electron microscopy (SEM) and energy-dispersive X-ray spectroscopy (EDS).

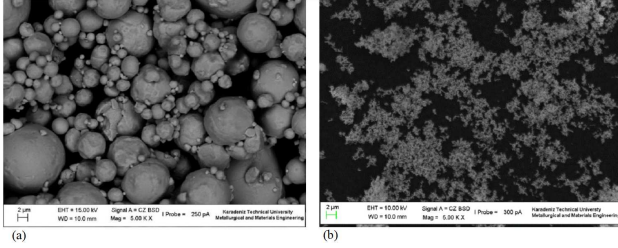


Fig. 1. Morphology of as received (a) Ag and (b)  $\text{SnO}_2$  powders.

### 3. Results and discussion

Grains of Ag powder have had a spherical shape (Fig. 1a), whereas those of  $\text{SnO}_2$  powder have had an irregular shape (Fig. 1b), from a morphological point of view. Besides,  $\text{SnO}_2$  powder has a smaller particle size than that of Ag powder. Figure 2 shows the morphological evolution of the  $\text{Ag}_8\text{SnO}_2$  powder mixture at different stages of milling process. In the early stages of the milling process, ductile Ag components were flattened by ball-to-powder collisions, mainly by cold welding. It can be seen from Fig. 2a–c that the cold welding event is dominant over fracturing and the particle size reduction is at an insignificant level throughout this period (Table I). This is the cause of the flaky Ag particles remaining in the powder morphology. The trails of fracturing have appeared after 7 h of milling (Fig. 2d–f) and the flaky powder particles have started to get fragmented into smaller pieces. As a consequence of this gradual refinement in powder particle size, average particle size was reduced to  $4.831 \mu\text{m}$  (Fig. 3).

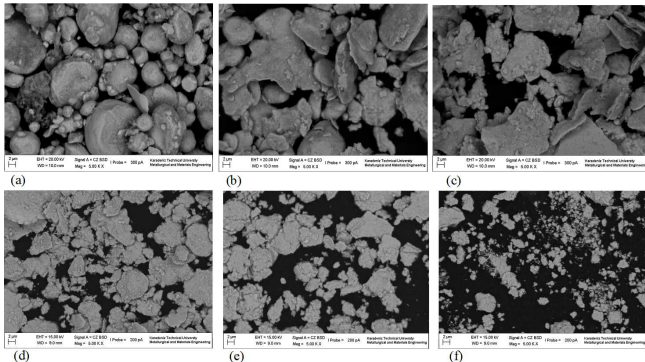


Fig. 2. Morphological evolution of the  $\text{Ag}_8\text{SnO}_2$  powder mixture after milling for (a) 0.5, (b) 2, (c) 4, (d) 7, (e) 16 and (f) 25 h.

TABLE I

Average particle size ( $d(0.5)$ , [ $\mu\text{m}$ ]) as a function of milling time (MT, [h]), for  $\text{Ag}_8\text{SnO}_2$  composite powder.

MT	0	0.5	2	4	7	10	16	20	25
$d(0.5)$	18.65	16.32	16.20	15.97	13.69	13.52	10.65	7.41	4.83

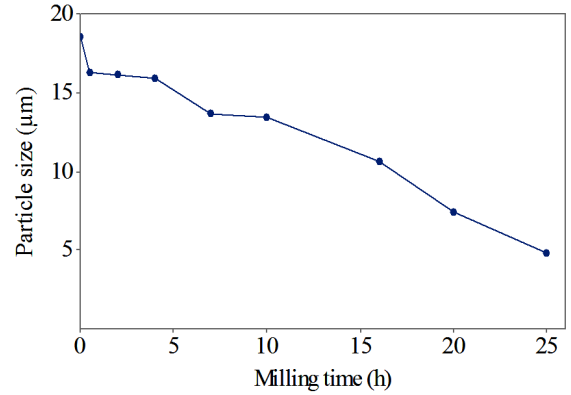


Fig. 3. Average particle size of the  $\text{Ag}_8\text{SnO}_2$  composite powder.

EDS mapping analysis, which contains back-scattered electron image (Fig. 4a), spectra (Fig. 4b) and the distribution of the elements in the mapping zone (Fig. 4c), was mainly performed on the green compact, to assess the homogeneity of the reinforcement particles in the matrix. Red, green and blue colors represent the distribution of the Ag, Sn and O elements in the selected mapping zone, respectively. It is clear from Fig. 4c that homogeneous distribution is obtained in the green compact, so the milling duration of 25 h is found to be sufficient. Prolonged milling duration promotes powder contamination, which is not desirable for electrical contact applications. Therefore, the powder mixture was not milled beyond 25 h.

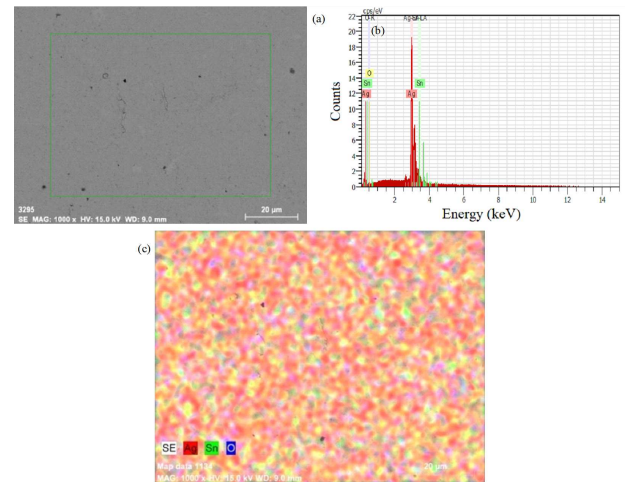


Fig. 4. EDS mapping analysis of the  $\text{Ag}_8\text{SnO}_2$  green compact, (a) back-scattered electron image of the mapping zone, (b) spectra in aforementioned zone, (c) distribution of the elements in the mapping zone.

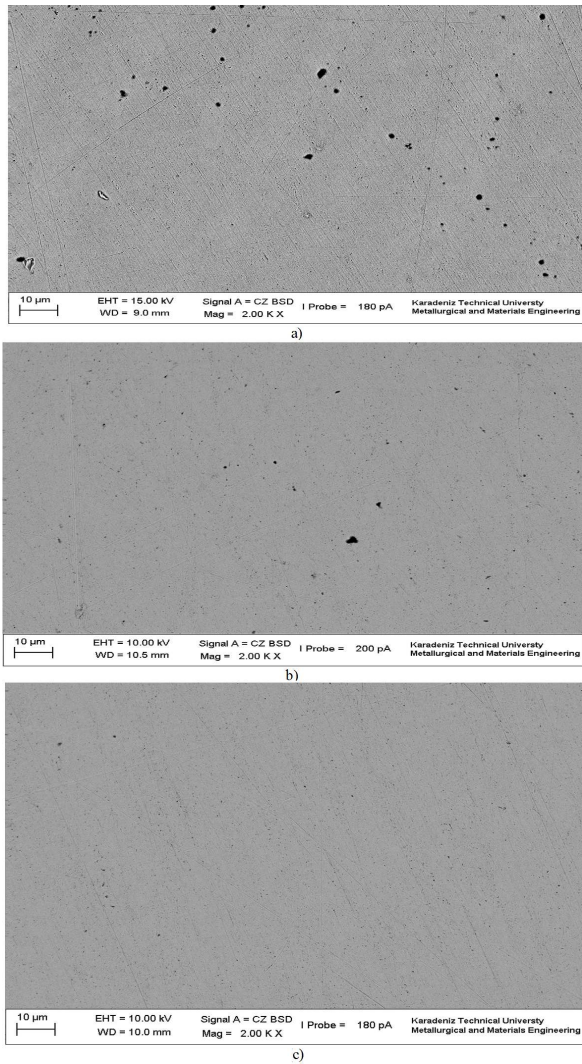


Fig. 5. Microstructure of the Ag8SnO<sub>2</sub> composites obtained by sintering at (a) 700, (b) 800 and (c) 900 °C.

The physical and mechanical properties of the composites for increasing sintering temperature are listed in Table II. The effect of different sintering regimes, namely temperatures of 700, 800 and 900 °C on the microstructure of the Ag8SnO<sub>2</sub> composites is shown in Fig. 5. Accordingly, the highest porosity value (3.17%) was observed in the specimens sintered at 700 °C (Fig. 5a). The amount of the porosity gradually decreases with increasing sintering temperature (Fig. 5b) and the minimum amount of porosity (1.59%) is obtained from the composites sintered at 900 °C (Fig. 5c). It was also found that the density and microhardness values of the composite had increased with increasing sintering temperature, and the maximum density (9.92 g/cm<sup>3</sup>) and microhardness values (78 HV) were obtained at sintering temperature of 900 °C (Table II).

Mass-loss values obtained from the arc-erosion tests are listed in Table III. Figure 6 shows the curves of the variation in the mass loss with the number of switching operations for both stationary and movable contacts.

TABLE II

Physical and mechanical properties of Ag8SnO<sub>2</sub> composites produced at increasing sintering temperature. Theoretical density, green density and green porosity of the samples were 10.08 g/cm<sup>3</sup>, 9.74 g/cm<sup>3</sup> and 3.37%, respectively

Sintering temperature [°C]	Sintered density [g/cm <sup>3</sup> ]	Sintered porosity [%]	Hardness (HV 0.1)
700	9.76	3.17	45
800	9.80	2.78	56
900	9.92	1.59	78

The mass loss in both types of contacts had increased with the increase in the number of switching operations. In addition, the mass loss in the stationary contacts was higher than that in the movable contacts.

TABLE III

Mass loss [mg] values of stationary and movable electrical contacts with increasing switching number for Ag8SnO<sub>2</sub>.

Type of contact	Switching number							
	5000	10000	15000	20000	25000	30000	35000	40000
Station.	8.26	15.90	22.25	27.09	29.74	33.69	37.28	39.28
Movable	5.57	9.93	12.72	15.76	18.26	20.80	23.01	26.52
Total	13.83	25.83	34.97	42.85	48.00	54.49	60.29	65.80

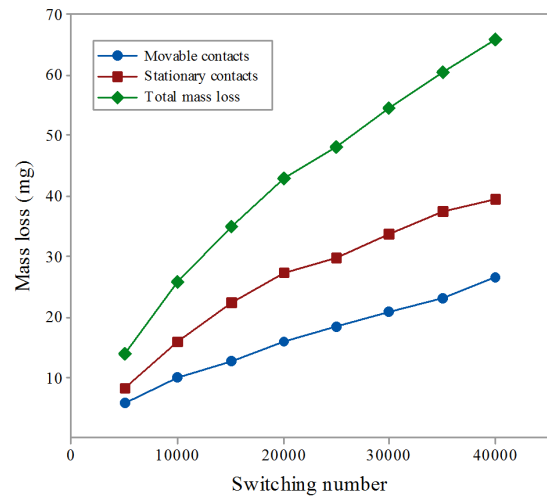


Fig. 6. Mass loss versus switching number for both stationary and movable contacts.

The mass loss during the initial stage constitutes a fairly high portion of the total mass loss, especially in the stationary contacts, due to the surface roughness characteristics of the contacts. In the first 5000 cycles, numerous cavities, microcrack trails and partly melted regions were observed at the surface of stationary contacts (Fig. 7a), whereas arc-originated particles were deposited on the surface of movable contacts (Fig. 7b). With



increasing operation number, some deep craters were formed on movable contacts (Fig. 7c–d). After 25 000 cycles, liquid metal had filled the voids on movable contacts (Fig. 7f) while shallow craters were observed on stationary ones (Fig. 7e). In the later stages of switching operations, some of the wear particles (Fig. 7h) were transformed from the movable contacts upon the craters of the stationary contacts (Fig. 7g).

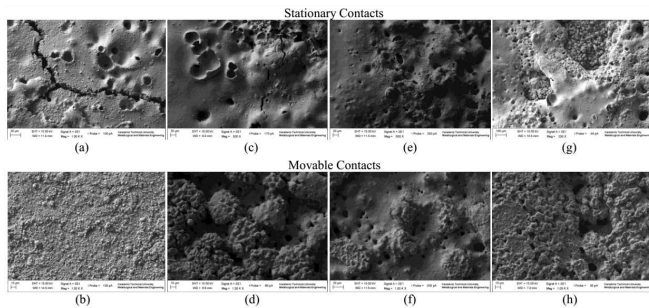


Fig. 7. SEM micrographs showing the surfaces of both contacts, tested at 20 A, for different switching numbers: (a, b) 5 000; (c, d) 20 000; (e, f) 25 000; (g, h) 40 000.

#### 4. Conclusions

Powder particle size has decreased with increasing milling time. Average particle size was reduced to 4.831  $\mu\text{m}$  after milling duration of 25 h. Fine and homogeneous distribution of the reinforcement particles ( $\text{SnO}_2$ ) in the Ag matrix was successfully provided by MA technique. Therefore, milling duration of 25 h was found sufficient to achieve homogenization and to inhibit powder contamination. Vacuum sintering was found to be advantageous to obtain composites with fairly low porosity (1.59%). The amount of porosity gradually decreases with increasing sintering temperature. Moreover, density and microhardness values increase with increasing sintering temperature. As a result, the optimal physical and mechanical properties were obtained from the specimens sintered at 900 °C. Therefore, optimum sintering temperature was determined to be 900 °C. The mass losses in both stationary and movable contacts have increased with the increase in the number of switching operations. Compared with the movable contacts, the stationary contacts exhibited a higher mass loss at up to 40 000 switching operations.

#### Acknowledgments

This work was supported by the Scientific Research Fund of Karadeniz Technical University (KTUBAP, Project No: 1073).

#### References

- [1] P.G. Slade, *Electrical Contacts: Principles and Applications*, CRC Press, Boca Raton 2014.
- [2] M. Braunovic, N.K. Myshkin, V.V. Konchits, *Electrical Contacts: Fundamentals, Applications and Technology*, CRC Press, Boca Raton 2006.
- [3] Z. Wei, L. Zhang, H. Yang, T. Shen, L. Chen, *J. Mater. Res.* **31**, 468 (2016).
- [4] B. Juszcyk, J. Kulasa, A. Gubernat, W. Malec, L. Ciura, M. Malara, L. Wierzbicki, J. Golebiewska-Kurzawska, *Arch. Metall. Mater.* **57**, 1063 (2012).
- [5] M. Zhang, X. Wang, X. Yang, J. Zou, S. Liang, *T. Nonferr. Metal. Soc. China* **26**, 783 (2016).
- [6] S. Biyik, M. Aydin, *Acta Phys. Pol. A* **127**, 1255 (2015).
- [7] S. Biyik, F. Arslan, M. Aydin, *J. Electron. Mater.* **44**, 457 (2015).
- [8] Q. Shi, J. Yang, W.X. Peng, J.Z. Dong, Y.Q. Chu, H. Tang, C.S. Li, *RSC Adv.* **5**, 100472 (2015).
- [9] J. Wang, W. Liu, D. Li, Y. Wang, *J. Alloy. Compd.* **588**, 378 (2014).
- [10] S. Biyik, M. Aydin, *Acta Phys. Pol. A* **129**, 656 (2016).
- [11] S. Biyik, M. Aydin, *Proc. IEEE 15th Int. Conf. on Thermal, Mechanical and Multi-Physics Simulation and Experiments in Microelectronics and Microsystems (EuroSimE)*, Ghent 2014, p. 1.